Preliminary Investigation of a Nonconforming Discontinuous Galerkin Method for Solving the Time-Domain Maxwell Equations

Hassan Fahs[1], Loula Fezoui[1], Stéphane Lanteri[1], and Francesca Rapetti[2]

[1]INRIA, 06902 Sophia Antipolis, France
[2]Nice/Sophia Antipolis University, J.A. Dieudonné Mathematics Lab., UMR CNRS 6621, 06108 Nice, France

This paper is concerned with the design of a high-order discontinuous Galerkin (DG) method for solving the 2-D time-domain Maxwell equations on nonconforming triangular meshes. The proposed DG method allows for using nonconforming meshes with arbitrary-level hanging nodes. This method combines a centered approximation for the evaluation of fluxes at the interface between neighboring elements of the mesh, with a leap-frog time integration scheme. Numerical experiments are presented which both validate the theoretical results and provide further insights regarding to the practical performance of the proposed DG method, particulary when nonconforming meshes are employed.

Index Terms—Discontinuous Galerkin method, Maxwell's equations, nonconforming triangular meshes.

I. INTRODUCTION

A LOT of methods have been developed for the numerical solution of the time-domain Maxwell equations. Finite-difference time-domain (FDTD) methods based on Yee's scheme [1] (a time explicit method defined on a staggered mesh) are still prominent because of their simplicity and their nondissipative nature (they hold an energy conservation property which is an important ingredient in the numerical simulation of unsteady wave propagation problems). Unfortunately, the discretization of objects with complex shapes or small geometrical details using cartesian meshes hardly yields an efficient numerical methodology. A natural approach to overcome this difficulty in the context of the FDTD method is to resort to nonconforming local refinement. However, instabilities have often been reported for these methods and rarely studied theoretically until very recently [2].

Finite-element methods can handle unstructured meshes and complex geometries. However, the development of high-order versions of such methods for solving Maxwell's equations has been relatively slow. A primary reason is the appearance of spurious, nonphysical solutions when a straightforward nodal continuous Galerkin finite-element scheme is used to approximate the Maxwell curl-curl equations. Bossavit made the fundamental observation that the use of special curl-conforming elements [3] could avoid the problem of spurious modes by mimicking properties of vector algebra [4].

In an attempt to offer an alternative to the classical finite-element formulation based on edge elements, we consider here discontinuous Galerkin formulations [5] based on high-order nodal elements for solving the first-order time-domain Maxwell's equations. Discontinuous Galerkin time-domain (DGTD) methods can handle unstructured meshes, deal with discontinuous coefficients and solutions, by locally varying polynomial order, and get rid of differential operators (and finite-element

mass matrices) by using Green's formula for the integration over control volumes. People rediscover indeed the abilities of these methods to handle complicated geometries, media and meshes, to achieve high-order accuracy by simply choosing suitable basis functions, to allow long-range time integrations and, last but not least, to remain highly parallelizable at the end. Whereas high-order discontinuous Galerkin time-domain methods have been developed on hexahedral [6] and tetrahedral [7] meshes, the design of nonconforming discontinuous Galerkin time-domain methods is still in its infancy. In practice, the nonconformity can result from a local refinement of the mesh (i.e., h-refinement), of the interpolation order (i.e., p-enrichment) or of both of them (i.e., hp-refinement).

The present study is a preliminary step towards the development of a nonconforming discontinuous Galerkin method for solving the three-dimensional time-domain Maxwell equations on unstructured tetrahedral meshes. Here, we consider the two-dimensional case and we concentrate on the situation where the discretization is locally refined in a nonconforming way yielding triangular meshes with arbitrary-level hanging nodes. In this context, the contributions of this work are on the one hand, a theoretical and numerical stability analysis of high-order DGTD methods on nonconforming triangular meshes and, on the other hand, a numerical assessment of the convergence of such DGTD methods.

II. DISCONTINUOUS GALERKIN TIME-DOMAIN METHOD

We consider the two-dimensional Maxwell equations in the TMz polarization on a bounded domain $\Omega \subset \mathbb{R}^2$

$$
\begin{cases}
\epsilon\frac{\partial E_z}{\partial t} - \frac{\partial H_y}{\partial x} + \frac{\partial H_x}{\partial y} = 0, \\
\mu\frac{\partial H_x}{\partial t} + \frac{\partial E_z}{\partial y} = 0, \quad \text{and} \quad \mu\frac{\partial H_y}{\partial t} - \frac{\partial E_z}{\partial x} = 0
\end{cases} \tag{1}
$$

where the unknowns are $\mathbf{E} = (0, 0, E_z)$ and $\mathbf{H} = (H_x, H_y, 0)$, the electric and magnetic fields, respectively. The electric permittivity ϵ and the magnetic permeability μ of the medium are assumed to be piecewise constant. We assume that the field components as well as the material parameters ϵ and μ do not depend on the z coordinate. The boundary $\partial\Omega$ is assumed to be a perfect electric conductor.

We consider a partition $\mathcal{T}_h$ of Ω into a set of triangles T_i of size h_i such that the mesh size $h = \max_{T_i \in \mathcal{T}_h} h_i$. To each $T_i \in \mathcal{T}_h$ we assign an integer $p_i > 0$ and we collect the p_i in the vector $p = \{p_i : T_i \in \mathcal{T}_h\}$. Within this construction we admit meshes with possibly hanging nodes, i.e., nonconforming meshes where triangle vertices can lie in the interior of edges of other triangles. Each triangle T_i is assumed to be the image, under a smooth bijective and affine mapping of a fixed master triangle $\hat{\mathrm{T}} = \{\hat{x}, \hat{y} \,|\, \hat{x}, \hat{y} \geq 0; \hat{x} + \hat{y} \leq 1\}$. In the following, we seek for approximate solutions to (1) in the finite dimensional space $V_p(\mathcal{T}_h) := \{v \in L^2(\Omega) : v_{|T_i} \in \mathbb{P}_{p_i}(T_i), \forall T_i \in \mathcal{T}_h\}$, where $\mathbb{P}_{p_i}(T_i)$ denotes the space of polynomials of total degree at most p_i on the element T_i. We denote by $\{\varphi_{ij}\}_{j=1}^{d_i}$ the local basis of functions spannning the space $V_p(\mathcal{T}_h)$ where d_i is the local number of degrees of freedom (dof). Note that the polynomial degree p_i may vary from element to element in the mesh and that a function $v_h^p \in V_p(\mathcal{T}_h)$ is discontinuous across element interfaces. For two distinct triangles T_i and T_k in $\mathcal{T}_h$, the intersection $T_i \cap T_k$ is an (oriented) edge s_{ik} which we will call interface, with oriented normal vector $\vec{n}_{ik}$. For the boundary interfaces, the index k corresponds to a fictitious element outside the domain. By nonconforming interface we mean an interface s_{ik} which has at least one of its two vertices in a hanging node or such that $p_i|_{s_{ik}} \neq p_k|_{s_{ik}}$ or both of them. Finally, we denote by $\mathcal{V}_i$ the set of indices of the elements neighboring T_i.

The DGTD method at the heart of this study is based on a leap-frog time scheme (E_z is computed at integer time-stations and H_x and H_y at half-integer time-stations) and totally centered numerical fluxes at the interface between elements. Decomposing H_x, H_y and E_z on element T_i according to

$$H_{\mathbf{x}}\left(\cdot, t^{n+\frac{1}{2}}\right) = \sum_{j=1}^{d_i} H_{\mathbf{x}_{ij}}^{n+\frac{1}{2}} \varphi_{ij}, \quad E_z(\cdot, t^n) = \sum_{j=1}^{d_i} E_{z_{ij}}^n \varphi_{ij}$$

where $\mathbf{x} \in \{x, y\}$. Using the notations $\mathbf{E}_{z_i}^n = (E_{z_{i1}}^n, \ldots, E_{z_{id_i}}^n)^t$ and $\mathbf{H}_{\mathbf{x}_i}^{n+(1/2)} = (H_{\mathbf{x}_{i1}}^{n+(1/2)}, \ldots, H_{\mathbf{x}_{id_i}}^{n+(1/2)})^t$, the DGTD-$\mathbb{P}_{p_i}$ method writes

$$\begin{cases} \epsilon_i \mathbb{M}_i \dfrac{\mathbf{E}_{z_i}^{n+1} - \mathbf{E}_{z_i}^n}{\Delta t} = -\mathbb{K}_i^x \mathbf{H}_{y_i}^{n+\frac{1}{2}} + \mathbb{K}_i^y \mathbf{H}_{x_i}^{n+\frac{1}{2}} \\ \quad + \sum_{k \in \mathcal{V}_i} \left(\mathbb{G}_{x_{ik}}^{n+\frac{1}{2}} - \mathbb{G}_{y_{ik}}^{n+\frac{1}{2}}\right), \\ \mu_i \mathbb{M}_i \dfrac{\mathbf{H}_{x_i}^{n+\frac{1}{2}} - \mathbf{H}_{x_i}^{n-\frac{1}{2}}}{\Delta t} = \mathbb{K}_i^y \mathbf{E}_{z_i}^n - \sum_{k \in \mathcal{V}_i} \mathbb{F}_{y_{ik}}^n, \\ \mu_i \mathbb{M}_i \dfrac{\mathbf{H}_{y_i}^{n+\frac{1}{2}} - \mathbf{H}_{y_i}^{n-\frac{1}{2}}}{\Delta t} = -\mathbb{K}_i^x \mathbf{E}_{z_i}^n + \sum_{k \in \mathcal{V}_i} \mathbb{F}_{x_{ik}}^n \end{cases}$$

where $\mathbb{M}_i$ is the local mass (symmetric positive definite) matrix, and $\mathbb{K}_i^{\mathbf{x}}$ is the (skew-symmetric) stiffness matrix. The vector quantities $\mathbb{F}_{\mathbf{x}_{ik}}^n$ and $\mathbb{G}_{\mathbf{x}_{ik}}^{n+(1/2)}$ are defined as

$$\mathbb{F}_{\mathbf{x}_{ik}}^n = \mathbb{S}_{ik}^{\mathbf{x}} \mathbf{E}_{z_k}^n, \quad \mathbb{G}_{\mathbf{x}_{ik}}^{n+\frac{1}{2}} = \mathbb{S}_{ik}^{\mathbf{x}} \mathbf{H}_{\mathbf{x}_k}^{n+\frac{1}{2}}$$

where $\mathbb{S}_{ik}^{\mathbf{x}}$ is the $d_i \times d_k$ interface matrix on s_{ik} which verifies ${}^t\mathbb{S}_{ik}^{\mathbf{x}} = -\mathbb{S}_{ki}^{\mathbf{x}}$ (if s_{ik} is an internal interface) and ${}^t\mathbb{S}_{ik}^{\mathbf{x}} = \mathbb{S}_{ik}^{\mathbf{x}}$ (if s_{ik} is a boundary interface). Note that, for nonconforming interfaces, we calculate the matrix $\mathbb{S}_{ik}^{\mathbf{x}}$ by using a Gaussian quadrature formula [8].

In [8], a numerical dispersion has been observed when a low-order conforming DGTD-$\mathbb{P}_p$ ($p = 0, 1$ and $p_i = p$ everywhere) is applied. This dispersion error is not reduced notably

TABLE I
NUMERICAL CFL OF THE DGTD-$\mathbb{P}_p$ METHOD

$p_c = p_f = p$	0	1	2	3	4
$\mathrm{CFL}_p^{\mathrm{num}}$	1.0	0.3	0.2	0.15	0.1

TABLE II
NUMERICAL CFL OF THE DGTD-$\mathbb{P}_{p_c}$:$\mathbb{P}_{p_f}$ METHOD

$p_c : p_f$	1:0	2:0	2:1	3:1	3:2	4:2
$\mathrm{CFL}_{p_c:p_f}^{\mathrm{num}}$	1.0	0.4	0.3	0.25	0.15	0.15

by using a h-refinement strategy (i.e., modifying h for a fixed p, yielding nonconforming locally refined meshes). On the other hand, the dispersion error is minimized when a p-enrichment strategy (i.e., modifying p for a fixed h) is used. However, the latter approach requires a large number of dof thus increases substantially the computing time and memory usage. We propose here a hp-like DGTD method where we combine h-refinement and p-enrichment strategies. This method consists in using a high polynomial order in the coarse (i.e., not refined) mesh and a low-order one in the refined region. The resulting scheme is referred to as a DGTD-$\mathbb{P}_{p_c}$:$\mathbb{P}_{p_f}$ method where p_c and p_f are the polynomial degrees in the coarse and fine elements respectively. This kind of scheme is a first step towards a fully adaptive hp-refinement method relying on appropriate error estimators.

III. STABILITY ANALYSIS

On any nonconforming mesh, the DGTD method exactly conserves the following energy [8]:

$$\mathcal{E}^n = \frac{1}{2} \sum_i \left(\epsilon_i {}^t\mathbf{E}_{z_i}^n \mathbb{M}_i \mathbf{E}_{z_i}^n + \mu_i {}^t\mathbf{H}_{x_i}^{n-\frac{1}{2}} \mathbb{M}_i \mathbf{H}_{x_i}^{n+\frac{1}{2}} \right.$$
$$\left. + \mu_i {}^t\mathbf{H}_{y_i}^{n-\frac{1}{2}} \mathbb{M}_i \mathbf{H}_{y_i}^{n+\frac{1}{2}} \right)$$

and one can show that $\mathcal{E}^n$ is a positive definite quadratic form of all numerical unknowns under the CFL-like sufficient stability condition on the time step Δt

$$\forall i, \forall k \in \mathcal{V}_i, \quad c_i \Delta t(2\alpha_i + \beta_{ik}) \leq 4 \min\left(\frac{|T_i|}{P_i^x}, \frac{|T_i|}{P_i^y}\right)$$

where c_i is the local speed of propagation, $|T_i|$ is the surface of T_i, and $P_i^{\mathbf{x}} = \sum_{k \in \mathcal{V}_i} |n_{ik\mathbf{x}}|$. The constants α_i and $\beta_{ik}(k \in \mathcal{V}_i)$ verify some inequalities [8] on T_i and s_{ik}

$$\begin{cases} \forall \xi_i \in \mathsf{Span}\{\varphi_{ij}, 1 \leq j \leq d_i\}, \mathbf{x} \in \{x, y\} \\ \left\|\frac{\partial \xi_i}{\partial \mathbf{x}}\right\|_{T_i} \leq \frac{\alpha_i P_i^{\mathbf{x}}}{|T_i|} \|\xi_i\|_{T_i}, \quad \|\xi_i\|_{s_{ik}}^2 \leq \beta_{ik} \frac{\|\vec{n}_{ik}\|}{|T_i|} \|\xi_i\|_{T_i}^2. \end{cases}$$

The values of α_i only depend on the local polynomial order p_i while the values of β_{ik} depend on p_i and on the number of hanging nodes in the interface s_{ik}. Consequently, if p_i and the number of hanging nodes increase, the theoretical CFL values become restrictive [8]. We report here on the CFL values evaluated numerically (i.e., by assessing the limit beyond which we observe a growth of the discrete energy). The corresponding values of $\mathrm{CFL}_{p_i}^{\mathrm{num}}$ are summarized in Tables I and II for the DGTD-$\mathbb{P}_{p_c}$:$\mathbb{P}_{p_f}$ and DGTD-$\mathbb{P}_p$ methods, respectively. One can
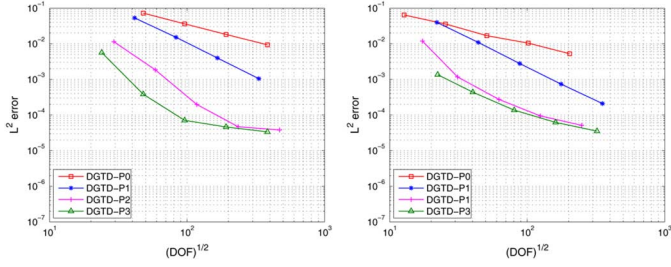
Fig. 1. Numerical convergence of the DGTD-$\mathbb{P}_p$ method with h-refinement. Nonconforming (left) and conforming (right) triangular mesh.
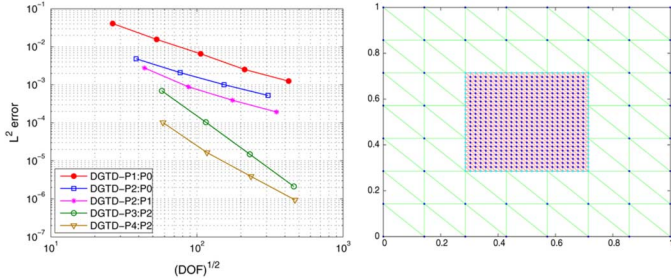

Fig. 2. Numerical convergence of the DGTD-$\mathbb{P}_{p_c}$:$\mathbb{P}_{p_f}$ method (left) on the nonconforming triangular mesh (right).

note that for $p_c = p_f + 1 = p + 1$, the DGTD-$\mathbb{P}_{p_c}$:$\mathbb{P}_{p_f}$ method has the same stability limit as the DGTD-$\mathbb{P}_p$ scheme, as long as the mesh is actually refined. This is not a surprise, since the DGTD-$\mathbb{P}_{p_c}$ scheme, which has a reduced stability domain, is only used on elements of the coarse mesh (which are at least twice larger than elements of the refined mesh).

IV. CONVERGENCE ANALYSIS

In [7] it is shown that the convergence order of the centered in space and time DGTD-$\mathbb{P}_p$ method, in the case of conforming simplicial meshes, is

$$\mathcal{O}\left(Th^{\min(s,p)}\right) + \mathcal{O}(\Delta t^2) \qquad (2)$$

where Δt is the time step over the interval $[0, T]$ and the solution belongs to $H^s(\Omega)$ with $s > 1/2$. Our attention is turned in the validity of this result in the case of nonconforming meshes using the DGTD-$\mathbb{P}_p$ and DGTD-$\mathbb{P}_{p_c}$:$\mathbb{P}_{p_f}$ methods, and a preliminary answer is given here on the basis of numerical simulations.

A. Eigenmode in a PEC Cavity Filled With Vacuum

The first test case that we consider is the propagation of an eigenmode in a unitary PEC cavity with $\epsilon = \mu = 1$ in normalized units. Numerical simulations make use of triangular meshes of the square $[0, 1] \times [0, 1]$ and nonconforming meshes are obtained thanks to local refinements of a rectangular zone as shown on Fig. 2, right. Figs. 1 and 2 illustrate respectively the numerical convergence of the DGTD-$\mathbb{P}_p$ and DGTD-$\mathbb{P}_{p_c}$:$\mathbb{P}_{p_f}$ methods using conforming and nonconforming triangular meshes, in terms of the evolution of the L^2-error as a function of the square root of the number of dof. These errors are

TABLE III
NUMERICAL CONVERGENCE OF THE DGTD-$\mathbb{P}_p$ METHOD

Conforming triangular mesh: convergence order.

Interpolation order p	0	1	2	3
Convergence order	0.90	1.90	1.98	1.37

Non-conforming triangular mesh: convergence order.

Interpolation order p	0	1	2	3
Convergence order	0.99	1.89	2.17	1.78

TABLE IV
NUMERICAL CONVERGENCE OF THE DGTD-$\mathbb{P}_{p_c}$:$\mathbb{P}_{p_f}$ METHOD

Non-conforming triangular mesh: convergence order.

Interpolation orders p_c:p_f	1:0	2:0	2:1	3:2	4:2
Convergence order	1.27	1.07	1.27	2.78	2.24

TABLE V
L^2 ERROR, CPU TIME (SECONDS), NUMBER OF dof AND NUMBER OF TIME STEPS MEASURED AFTER TWO PERIODS

DGTD-$\mathbb{P}_p$: Conforming triangular mesh.

p	1	2	3
L^2 error, CPU	2.78E-03, 10	5.13E-05, 324	3.53E-05, 658
# dof, #Δt	7740, 600	61500, 4800	102400, 7200

DGTD-$\mathbb{P}_p$: Non-conforming triangular mesh.

p	1	2	3
L^2 error, CPU	3.98E-03, 154	4.69E-05, 580	4.61E-05, 489
# dof, #Δt	27552, 3200	55224, 6400	36860, 6400

DGTD-$\mathbb{P}_{p_c}$:$\mathbb{P}_{p_f}$: Non-conforming triangular mesh.

p_c:p_f	2:1	3:2	4:2
L^2 error, CPU	2.78E-03, 2	4.56E-05, 79	1.66E-05, 51
# dof, #Δt	1935, 625	24024, 2156	13690, 2400

measured after two periods. Corresponding asymptotic convergence orders are summarized in Tables III and IV. As it could be expected from the use of a second-order accurate time integration scheme, the asymptotic convergence order is bounded above by 2 independently of the interpolation order p (except for $p = 2 = p_f$ on nonconforming mesh for which we obtain convergence orders higher than 2) and higher order convergence rates will require more accurate time integration schemes. Furthermore, we can observe that for $p = 0, 1$, the convergence order is $\mathcal{O}(h^{p+1})$. From these points of view, it seems that the formula (2) is suboptimal and suggests that theoretical convergence study conducted in [7] might be improved in view of the development of h- and hp-adaptive DGTD methods. Moreover, we have observed in the case of DGTD-$\mathbb{P}_{p_c}$:$\mathbb{P}_{p_f}$ method that it is not necessary to increase p_c to more than $p_f + 2$, since the convergence order is not improved.

Table V shows the CPU times, the L^2 errors, the number of time steps (#Δt), and the number of dof (# dof) for some cases of the proposed methods. One can see that to achieve a given accuracy the gains of CPU time and memory consumption is notable if we use the DGTD-$\mathbb{P}_{p_c}$:$\mathbb{P}_{p_f}$ method. Moreover, to reach a high accuracy, the cost of the nonconforming DGTD-$\mathbb{P}_p$ method is comparable with the conforming one.
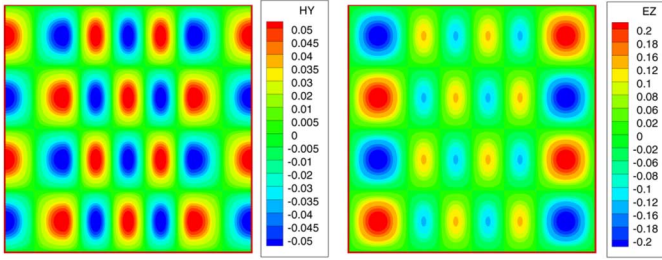
Fig. 3. Eigenmode in a PEC cavity containing a lossless material.

TABLE VI
NUMERICAL CONVERGENCE OF THE DGTD-$\mathbb{P}_p$ METHOD

Conforming triangular mesh: convergence order.

Interpolation order p	0	1	2	3
Convergence order	0.81	0.85	0.44	0.37

Non-conforming triangular mesh: convergence order.

Interpolation order p	0	1	2	3
Convergence order	0.85	0.82	0.36	0.34

TABLE VII
NUMERICAL CONVERGENCE OF THE DGTD-$\mathbb{P}_{p_c}$:$\mathbb{P}_{p_f}$ METHOD

Non-conforming triangular mesh: convergence order.

Interpolation orders p_c:p_f	1:0	2:0	3:0	2:1	3:1
Convergence order	0.95	1.03	0.91	0.90	0.98

B. Eigenmode in a PEC Cavity With a Dielectric Material

In this problem, a lossless dielectric with a relative permittivity ϵ_2 is enclosed by air in the x direction, and the media are homogeneous along the y direction and nonmagnetic. The computational domain $\Omega = \{(x, y), |x| \leq 1, |y| \leq 1\}$ is enveloped by PEC walls. The permittivity is given as $\epsilon = \epsilon_1$ if $(1)/(2) \leq |x| \leq 1$ and $|y| \leq 1$, and $\epsilon = \epsilon_2$ if $|x| \leq (1)/(2)$ and $|y| \leq 1$, where $\epsilon_1 = 1$ and $\epsilon_2 = 2.25$. An analytical solution for time varying electromagnetic fields is known for this problem [9]. Contour lines of the H_y and E_z components at time $t = 1.0$ are shown in Fig. 3. The nonconforming meshes are obtained by refining the heterogeneous zone. Numerical convergence orders measured at time $t = 0.65$ are summarized in Tables VI and VII. One can note that the convergence of the DGTD-$\mathbb{P}_p(p \geq 2)$ method is notably slower than what was observed with the previous test case, which is the result of the presence of a material interface in the domain. On the other hand, Table VII shows that the convergence rate is improved with the DGTD-$\mathbb{P}_{p_c}$:$\mathbb{P}_{p_f}$ method using a low interpolation order in the heterogenuous zone.

Table VIII shows the CPU times, the number of dof and the number of time steps to achieve a prescribed error level. The results of the DGTD-$\mathbb{P}_{p_c}$:$\mathbb{P}_{p_f}$ on nonconforming meshes are very satisfactory comparing with the conforming DGTD-$\mathbb{P}_p$ method.

TABLE VIII
CPU TIME (SECONDS), NUMBER OF DOF AND NUMBER OF TIME STEPS TO ACHIEVE AN ERROR OF 3.0E-03 AT $t = 1.0$

DGTD-$\mathbb{P}_p$: Conforming triangular mesh.

p	0	1	2	3
# dof	352800	194400	76800	32000
#Δt, CPU	194, 290	276, 110	246, 41	184, 12

DGTD-$\mathbb{P}_{p_c}$:$\mathbb{P}_{p_f}$: Non-conforming triangular mesh.

p_c:p_f	2:0	2:1	3:1	3:2
# dof	86016	180000	140800	54400
#Δt, CPU	368, 102	307, 130	295, 96	246, 29

V. CONCLUDING REMARKS AND FUTURE WORKS

We have presented preliminary results concerning a nonconforming discontinuous Galerkin method designed on unstructured triangular meshes for solving the time-domain Maxwell equations. The nonconformity is linked either to the use of locally refined meshes with an arbitrary-level of hanging nodes (i.e., h-refinement), or to the use of a space varying interpolation order (i.e., p-enrichment), or a combination of both (i.e., hp-refinement). Ongoing works target the extension to the numerical resolution of the 3-D time-domain Maxwell equations considering unstructured tetrahedral meshes.

REFERENCES

[1] K. Yee, "Numerical solution of initial boundary value problems involving Maxwell's equations in isotropic media," *IEEE Trans. Antennas Propag.*, vol. 14, no. 3, pp. 302–307, 1966.
[2] F. Collino, T. Fouquet, and P. Joly, "Conservative space-time mesh refinement methods for the FDTD solution of Maxwell's equations," *J. Comp. Phys.*, vol. 211, no. 1, pp. 9–35, 2006.
[3] J. C. Nedelec, "A new family of mixed finite elements in $\mathbb{R}^3$," *Numer. Math.*, vol. 50, pp. 57–81, 1986.
[4] A. Bossavit, "Solving Maxwell equations in a closed cavity, and the question of spurious modes," *IEEE Trans. Magn.*, vol. 26, no. 2, pp. 702–705, Mar. 1990.
[5] B. Cockburn, G. Karniadakis, and C. Shu, *Discontinuous Galerkin Methods. Theory, Computation and Applications*, ser. Lecture Notes in Computational Science and Engineering. New York: Springer-Verlag, 2000, vol. 11.
[6] G. Cohen, X. Ferrieres, and S. Pernet, "A spatial high spatial order hexahedral discontinuous Galerkin method to solve Maxwell's equations in time domain," *J. Comp. Phys.*, vol. 217, no. 2, pp. 340–363, 2006.
[7] L. Fezoui, S. Lanteri, S. Lohrengel, and S. Piperno, "Convergence and stability of a discontinuous Galerkin time-domain method for the heterogeneous Maxwell equations on unstructured meshes," *ESAIM: Math. Model. Numer. Anal.*, vol. 39, no. 6, pp. 1149–1176, 2006.
[8] H. Fahs, S. Lanteri, and F. Rapetti, "A hp-like discontinuous Galerkin method for solving the 2D time-domain Maxwell's equations on non-conforming locally refined triangular meshes," INRIA, Research Reports 6023 and 6162, 2007 [Online]. Available: http://hal.inria.fr/inria-00140783/
[9] S. Zhao and G. W. Wei, "High-order FDTD methods via derivative matching for Maxwell's equations with material interfaces," *J. Comp. Phys.*, vol. 200, no. 1, pp. 60–103, 2004.